Görgun, E., Zang, A., Bohnhoff, M., Milkereit, C., Dresen, G. (2009): Analysis of Izmit aftershocks 25 days before the November 12th 1999 Düzce earthquake, Turkey. - Tectonophysics, 474, 3-4, 507-515

DOI: 10.1016/j.tecto.2009.04.027

Analysis of Izmit aftershocks 25 days before the November 12th 1999 Düzce earthquake, Turkey

E. Görgün, A. Zang, M. Bohnhoff, C. Milkereit, G. Dresen

Helmholtz Centre Potsdam GFZ German Research Centre for Geosciences, Telegrafenberg, 14473 Potsdam/Germany.

Submitted to Tectonophysics

Abstract

We investigate spatial clustering of 2414 aftershocks along the Izmit M_w = 7.4 August 17, 1999 earthquake rupture zone. 25 days prior to the Düzce earthquake M_w = 7.2 (November 12, 1999), we analyze two spatial clusters, namely Sakarya (SC) and Karadere-Düzce (KDC). We determine the earthquake frequency-magnitude distribution (*b*-value) for both clusters. We find two high *b*-value zones in SC and one high *b*-value zone in KDC which are in agreement with large coseismic surface displacements along the Izmit rupture. The *b*-values are significantly lower at the eastern end of the Izmit rupture where the Düzce mainshock occurred. These low *b*-values at depth are correlated with low postseismic slip rate and positive Coloumb stress change along KDC. Since low *b*-values are hypothesized with high stress levels, we propose that at the depth of the Düzce hypocenter (12.5 km), earthquakes are triggered at higher stresses compared to shallower crustal earthquake. The decrease in *b*-value from the Karadere segment towards the Düzce Basin supports this low *b*-value high stress hypothesis at the eastern end of the Izmit rupture.

Key words: Düzce earthquake, fault asperities, Gutenberg-Richter law, Izmit earthquake, North Anatolian Fault Zone.

1. Introduction

The North Anatolian Fault Zone (NAFZ) is one of the seismically most active strike-slip faults world-wide extending 1600 km from eastern Anatolia to the north Aegean Sea (Figure 1a). The direction of slip corresponds well with Global Positioning System (GPS) derived 20 to 25 mm yr^{-1} westward motion of the Anatolian block with respect to Eurasia (McClusky et al., 2000; Reilinger et al., 2006). The Izmit earthquake of 17 August 1999 M_w = 7.4 exhibits a maximum surface displacement of 5.2 m at the Sapanca-Akyazi segment (Barka et al., 2002, Figure 1b). Average coseismic slip obtained from teleseismic waveform inversion is 2.5 m (Tibi et al., 2001) and 2.9 m from strong motion records (Bouchon et al., 2002). Synthetic Aperture Radar interferometry (InSAR) data inversion (Wright et al., 2001) shows a maximum displacement of approximately 5 m near the mainshock and a total coseismic moment of 2.6×10^{20} Nm. GPS data by Reilinger et al. (2000) indicate a geodetic coseismic moment of $M_0 = 1.7\times10^{20}$ Nm and a maximum displacement at the Izmit segment of about 5.7 m. Delouis et al. (2002) identified four segments along the Izmit rupture by using combined GPS, SAR, teleseismic and strong motion data.

Lay and Kanamori (1980) studied body waves and surface waves of large earthquakes in the Solomon Islands region in an attempt to determine the stress distribution on the thrust plane. They found that relatively short-period seismic body waves are radiated from only small parts of the entire rupture plane, which generates longer-period surface waves and over which the aftershocks occur. They interpreted the results in terms of an asperity model. This asperity model is an outgrowth of laboratory experiments on rock friction. Byerlee (1970), Scholz and Engelder (1976) suggested that

two sides of a fault are held together by areas of high strength, which they termed asperities. Extending this model to earthquake faults, Lay and Kanamori (1981) called the areas on the fault plane from where relatively short-period seismic body waves are radiated the fault asperities; it is assumed that the stronger spots are responsible for high-frequency seismic radiation.

From rock-deformation experiments in the laboratory three stages in acoustic emission fingerprints characterizing the failure of asperities are observed (Lei, 2003). During the first loading stage, the event rate which increases is documented by the inverse Omori law (Utsu, 1961). Simultaneously the *b*-value sharply decreases at the edge of the asperity. In the second stage prior to the mainshock, large magnitude events appear at the edge of the asperity (very close to the first stage hypocenters). During the third stage, significant increase and subsequent gradual decrease of *b*-value is observed along with a decreasing event rate (Zang et al., 1998).

In microscale and macroscale environments the *b*-value seems to rely on crack or rupture densities, which themselves result from the amount of applied stress or pressure, type of material, and rupture dynamics. Wiemer and Katsumata (1999) presented a "rupture mechanics approach" that relates *b*-values, coseismic slip and stress drop. Prior to an earthquake they suggest that areas subjected to high stress show low *b*-values. According to this approach high slip regions correspond to regions of high stress drop and high *b*-values of aftershocks. In this approach calculated slip distributions based on seismological and geodetic records of the mainshock are related to the aftershock seismicity parameters *b*-values. Sobiesiak et al. (2007) suggested that inhomogeneities in seismogenic fault areas can be mapped using *b*-value. These areas can be attributed to

potential asperities. Wiemer and Wyss (1997) described that areas of low *b*-values with a size range of 5 – 15 km correlate with asperities in the Parkfield and Morgan Hill sections of the San Andreas Fault (SAF). This hypothesizes that low *b*-values indicate asperities on the fault prior to a large earthquake is supported by the study of Wyss et al. (2004) showing that *b*-values on locked patches of the SAF near Parkfield are systematically lower than *b*-values on creeping patches. This observation is a direct consequence of the inverse relationship of *b*-value to the applied shear stress. Amitrano (2003) and Schorlemmer et al. (2005) show that the high-stress environment of locked fault patches is more likely to support future large earthquake occurrence. Westerhaus et al. (2002) analyzed SABONET (Sapanca-BOlu NETwork) data before the Izmit earthquake. The lowest *b*-values (~0.8) were located at the fault bend which runs through the epicenter of the 1999 Izmit mainshock. At the bend, a localized stress concentration is expected from numerical models of seismicity along asperities. The site of lowest *b*-values had been considered to be the most likely place for a major earthquake, a conclusion that was confirmed by the Izmit earthquake, with epicenter located about 13 km from the anticipated site. Aktar et al. (2004) who analyzed the first 45 days of the Izmit aftershock sequence detected three zones of relatively high *b*-values, two of which coincide with asperities revealed by Bouchon et al. (2002). Aktar et al. (2004) mainly focused on the area between the Yalova and Karadere segments (see Figure 1) and their analysis ended 42 days before the Düzce earthquake occurred. In this study we focus on the eastern part of the Izmit rupture (Sakarya, Karadere and Düzce regions). We discuss the Izmit aftershock sequence between October 18, 1999 and November 12, 1999 (i.e. the 25 days prior to the Düzce mainshock M_w =7.2). We analyze spatial variations of 2414

aftershocks with errors < 5 km (horizontal and vertical). Variations in *b*-values along the rupture and with depth are compared with stress level change and postseismic slip distribution, and are discussed in the context with the preparation process of the Düzce earthquake.

2. Data and Method

We focus on recordings obtained by a 15-station seismic network covering the Sakarya, Karadere and Düzce segments of Izmit rupture zone (Figure 2a). A long-term seismic network consisting of 15 stations (Figure 2a, yellow triangles) has been in operation since 1996 [SABONET, (SApanca-BOlu NETwork, Milkereit et al., 2000; Westerhaus et al., 2002)]. Figure 2a and 2b show 2414 of aftershock epicenters and hypocenters along the rupture zone, respectively (Bohnhoff et al., 2007).

Local magnitudes (M_l) were calculated following Baumbach et al. (2003) who developed a procedure to determine M_l for NW Turkey that was refined by Bindi et al. (2007) based on an updated attenuation curve and refined station corrections. The procedure involves an automatic estimation of M_l for all events at each station deconvolving the traces to synthetic Wood-Anderson torsion seismograms using instrument response and maximum horizontal peak amplitudes.

The frequency-magnitude distribution [Eq. (1)] describes the relationship between the frequency of occurrence and the magnitude of earthquakes (Ishimoto and Iida, 1939; Gutenberg and Richter, 1944):

$$\log_{10} N(M) = a - bM, \tag{1}$$

where *N(M)* refers to the frequency of earthquakes with magnitudes larger or equal than *M*. In a semi-logarithmic plot, the constants *a* (zero-offset) and *b* (slope) can be determined. The slope *b* has been interpreted to indicate the presence of asperity, stress and material heterogeneities along the fault plane (Mogi, 1962; Scholz, 1968; Amitrano, 2003; Schorlemmer et al., 2005).

The *b*-value is calculated using the maximum likelihood method published by Utsu (1966, 1999).

$$b = \frac{\log_{10}(e)}{\left[\langle M \rangle - \left(M_c - \Delta M_{bin}/2\right)\right]}. \qquad (2)$$

Here $\langle M \rangle$ is the mean of the binned magnitudes, M_c is the magnitude of completeness and ΔM_{bin} is the binning width of the catalogue [Eq. (2)].

An important issue in assessing data quality is the magnitude of completeness, M_c. Figure 3a depicts how the M_c level varies with time for the entire catalog. The completeness level ranges from 0.4 to 1.0. We compute the M_c threshold automatically for each nodal point, using the change of the slope of the magnitude curve (Wiemer, 2001). To ensure a robust estimation of *b*-values, we also restrict the catalog to events above the fixed level of M_c value (1.5) for *b*-values over the entire range of space and time. We observe that *b*-values do not change significantly in this case.

The *b*-value variations are calculated using the public software package ZMAP by Wiemer (2001). For sampling of earthquakes, we use cylindrical volumes perpendicular to the cross-sectional plane and centered at the nodes spaced at 1 km × 1 km. The length

of these cylindrical volumes is defined by the width of the volume along the cross section, which is 5 km. In each sample, we also require a minimum number of events with $M \geq M_c$, N_{min}, in order to determine reliable *b*-value. For samples containing fewer than N_{min} events, we do not compute *b*-values. Here, we arbitrarily set $N_{min} = 50$, because below this value the uncertainty in *b*-value increases rapidly (Wiemer and Wyss, 2002; Schorlemmer et al., 2004). The *b*-values are calculated in map view (Figure 4b) and as depth section (Figure 5b).

We use a bootstrap approach to estimate errors in *b* and M_c (Chernick, 1999). At every grid node we draw its detected number of events from its population, allowing any events to be selected more than once. From these events we compute M_c and b for $M \geq M_c$ and repeat this for every grid node 500 times. We then estimate the errors the standard deviation of *b*-values, taking into account the imperfection of the local frequency-magnitude distribution map view (Figure 4a) and depth section (Figure 5a) [Schorlemmer et al., 2003; Woessner and Wiemer, 2005].

3. Results

3.1. Sakarya Cluster

Figure 4b shows *b*-values in map view varying from 0.6 to 1.4 along the Izmit rupture zone. The *b*-value distribution (Figure 4b) shows strong spatial distributions in the Sakarya Cluster (SC). Different anomalous patches along this cluster can be distinguished. At region A in Figure 4b, high *b*-values (1.31) correlate with high coseismic displacements from field observations by Barka et al. (2002). At region B in Figure 4b, we find very low *b*-values at the intersection of Karadere-Düzce Cluster

(KDC) and SC. We compare the *b*-values for both regions and find a factor of two difference (Figure 4c, left). The low *b*-value zone (region B in Figure 4b) extends from northeast of SC to Karadere segment. This very low b-value (0.65) zone may be locked or high stress concentrated. At SC we identify a volume with high *b*-values extending to a depth of 12 km (Figure 5b). The frequency-magnitude distributions based on the catalog for asperities in the SC illustrate the large *b*-value contrast located in two volumes which are in the middle and southeast of SC. In these regions, the *b*-values vary from 1.2 to 1.4. For the catalog we obtain errors of 0.05 – 0.25. In the shallow and active parts, we observed errors of about 0.2 – 0.25 units, decreasing with depth and having a maximum in the high *b*-value region (Figure 4a and 5a).

The average *b*-value of aftershocks as a function of depth between October 17 – November 12, 1999 indicate $b = 1.0$ at 4 km depth and decreases gradually to $b = 0.6$ at ~ 6 km depth. At greater depth *b*-value increases to $b = 1.1$ at 9 km depth (Figure 6a). A second minimum of *b*-value ($b = 0.9$) is evident at along 10 km depth (Figure 6a).

3.2. Karadere-Düzce Cluster

Map of the spatial distribution of the *b*-values is computed using Izmit aftershocks for period 25 days before the Düzce mainshock (November 12, 1999 M_w =7.2). The high density of aftershocks within the Karadere-Düzce Cluster (KDC) is observed east of KDC (Düzce Basin) (30.95° – 31.15° in Figure 4b). The Karadere segment (30.78 – 30.94 in Figure 4b) has less activity than the Düzce Basin. Within the Izmit aftershock sequence, these two regions of high activity are revealed by SABONET data (Figure 2a and 2b), particularly at the eastern end of the Izmit rupture in the Düzce Basin. The

highest *b*-values (region C in Figure 4b) are found in the Karadere segment. The lowest *b*-values are found in the Düzce Basin (Figure 4b, region D). A comparison of *b*-values for regions C and D are shown in Figure 4c (right). The difference in *b*-value is significant (0.27). Region C coincides with 1.5 m surface slip (Barka et al., 2002) during the Izmit mainshock. No surface slip was observed in Düzce Basin before the Düzce mainshock on 12 November 1999. According to our results low *b*-values can be related to high Coulomb stress increase in this region (Utkucu et al., 2003). The Düzce Basin is characterized by low *b*-values (0.6) (see Figure 5b cross-section). For comparison we plot the postseismic slip inversion derived by GPS (Bürgmann et al., 2002) 25 days before the Düzce earthquake (Figure 5c). 25 days prior to the Düzce mainshock postseismic slip is very low (around 0 m) especially upper crust (above 20 km). Low postseismic slip in Düzce Basin correlates with low *b*-values (Figure 5b and 5c). In Düzce Basin we observed standard deviations of about 0.05 – 0.15 units for *b*-values (Figure 5a).

We calculate *b*-value variations as a function of depth at KDC (Figure 6b) using vertically sliding windows with 50 events. Horizontal error bars indicate the standard deviation while vertical bars indicate the width of the sliding window. The *b*-value is ≈ 0.8 at 4.5 km depth. Below 7 km depth the *b*-value gradually decreases from $b \approx 1.0$ to $b \approx 0.7$ up to 12 km depth. Below 12 km depth again *b*-value decreases from 1.0 to 0.8. Again, the double minimum of the depth variation of *b*-value as evident from SC (Figure 6a) is also visible at KDC (Figure 6b). Hypocentral depth of the Düzce earthquake is 12.5 km. This depth seems to correlate with *b*-value decrease (Figure 6b).

4. Discussion

The *b*-values along the Izmit rupture of the NAFZ vary significantly. High *b*-values at the middle of SC coincide with the maximum surface displacement observed (Figure 1b and 4b). Southeast of SC, *b*-values are high since this region spreads into the Mudurnu Valley fault where the 1967 earthquake (M_s = 7.2) occurred (Barka, 1996). There is one region found with high *b*-values at KDC. This region is associated with the Karadere segment (1.5 m surface displacement).

When mapping spatial variability in *b*-value one has to balance available resolution, with uncertainty in estimate and size of the seismotectonic feature in question. Schorlemmer et al. (2004) investigated *b*-value using a sampling radius ranging from 2 – 20 km. They suggested that sampling with radius > 5 km mixes populations of dissimilar frequency-magnitude distributions and thus cannot resolve the apparent real structure. For radius < 5 km no significant additional heterogeneity of *b*-values is detected. We conclude that a radius in the range of 4-5 km is the best choice for this fault segment and data set for identifying and resolving contrasts in *b*-values.

Schorlemmer and Wiemer (2005) found that prior to an earthquake low *b*-values correlate with high stress and low slip of unruptured areas. Taken together this suggests that drastic temporal changes in *b*-values may occur locally around asperities. Low *b*-values in some areas prior to a major seismic event can be followed by high *b*-values after the rupture occurred. The change in *b*-value indicates a coseismic stress drop if *b*-value is used as a stress-meter as suggested by Zang et al. (1998), Lei (2003), Schorlemmer and Wiemer (2005).

The exact spatial extension of the Izmit rupture to either end, i.e. below the Sea of Marmara and in the Düzce Basin is still a matter of debate. GPS results indicate that the western end of the Izmit rupture extended well into the Izmit Bay up to 20 km west of the Hersek Delta and may have ended SE of the Princes Islands (Karabulut et al., 2002). At the eastern end of the rupture it remains unclear if the rupture below the surface stopped on the Karadere fault or extended into the Düzce Basin (Reilinger et al., 2000; Wright et al., 2001; Bürgmann et al., 2002; Delouis et al., 2002; Pucci et al., 2006). The hypocenter catalog of Izmit aftershocks presented here indicates a sharp termination of activity towards the eastern end of the rupture (Figure 2b) where the Düzce earthquake initiated 87 days later (Bohnhoff et al., 2007; Bulut et al., 2007). This boundary correlates with low *b*-values (Figure 5b).

In laboratory studies (Scholz, 1968; Zang et al., 1998; Lei, 2003) and a variety of tectonic regimes (Wiemer and Katsumata, 1999; Schorlemmer et al., 2005) the frequency-magnitude distribution has been shown to be perturbed by stress and material heterogeneity. Both parameters are very heterogeneous along the Izmit rupture zone. It is conceivable that near the largest slip release the applied shear stress drops significantly during the mainshock, favoring a higher *b*-value for the aftershocks (Wiemer and Katsumata, 1999). For the Izmit aftershock sequence, we observe high *b*-values (= 1.31) near large surface displacements (= 5.2 m) as indicated by region A in Figure 4b (left) and Karadere segment (= 1.5 m) by region C in Figure 4b (right).

Areas subjected to high applied shear stresses are consistent with the observed low *b*-values. This is also compatible with observations of lower *b*-values at highly stressed asperities (Öncel and Wyss, 2000; Westerhaus et al., 2002; Schorlemmer and

Wiemer, 2005). We observe low *b*-values in the Düzce Basin prior to the Düzce mainshock. This observation indicates that the Düzce epicenter area is consistent with the model of Wiemer and Katsumata (1999) which would predict low *b*-values.

The most likely interpretation of our observation of low *b*-values at the eastern rim of the Izmit aftershock activity is based on the argument that the Izmit earthquake already ruptured parts of the Düzce fault segment. Comparing the location of our Izmit aftershocks at the eastern end of the rupture (Figure 7) with the observed surface rupture of the Düzce earthquake (Figure 7, blue line, from Pucci et al., 2006), it is apparent that half of the Düzce rupture was seismically active already in the Izmit aftershocks sequence.

For Düzce Basin, we find that areas showing low *b*-values are related to reduced postseismic slip (Figure 5c) within the uppermost 20 km of the Düzce Basin. According to time dependent afterslip studies, slip migrates from the Izmit mainshock area to the east (Reilinger et al., 2000; Bürgmann et al., 2002). We observe that *b*-values are gradually decreasing from 7 to 11.5 km depth (Figure 6b). The low *b*-values demonstrated here to occur between 7 and 11.5 km depth beneath the KDC suggest a stress concentrator. The depth of the Düzce mainshock (12.5 km) corresponds to within 1 km this stress concentrator. Slip is very low (~ 0 m) above 20 km (Figure 5c). At Düzce Basin low *b*-values at depth correlate with low postseismic slip.

The surface rupture associated with the Düzce earthquake follows the southern boundary of Düzce Basin and re-ruptured half of the part ruptured by the Izmit mainshock. The time span between the first Izmit aftershocks and the Düzce earthquake was 87 days and incorporate the preparation stage of Düzce mainshock. The rupture

plane of Düzce earthquake experienced a positive Coulomb stress change and this is clearly consistent with Coulomb triggering (Utkucu et al., 2003). Small aftershocks are important role in preparing a fault zone for failure (Steacy and McCloskey, 1998). In this context we speculate that the time to failure interval is characterized by migration of Izmit aftershocks towards Düzce. Late Izmit aftershocks are found to be pioneer earthquakes of the Düzce rupture. Analysis of *b*-value at Düzce Basin reveals that low *b*-values and low postseismic slips coincide with the sharp boundary of aftershocks determined 25 days prior to the Düzce mainshock.

5. Conclusions

By investigating the spatial variations of 2414 aftershocks of the 1999 Izmit earthquake using recordings from a 15-station seismic network covering the Sakarya, Karadere and Düzce regions we found the following conclusions.

Analyzing *b*-values in space, we identify three asperity regions along the Izmit segment of the North Anatolian Fault zone (Figure 8). High *b*-values (≥ 1.2) were found in the region middle (Asperity 1) and southeast (Asperity 2) of Sakarya Cluster, as well as in the region at the Karadere (Asperity 3) fault. Our observation is in agreement with the Wiemer and Katsumata (1999) rupture model where high slip corresponds to high *b*-value in the asperity region.

Low *b*-values in the Düzce Basin correlate with low postseismic slip derived from GPS. The change of *b*-value with depth in Sakarya Cluster is different from Karadere-Düzce Cluster. Lowest b-value in SC is $b \approx 0.7$ at 5.5 km depth. Lowest b-value in KDC is $b \approx 0.7$ at 11.5 km depth.

Pioneer earthquakes (late Izmit aftershocks) at the eastern end of the Izmit rupture indicate that half of the rupture plane activated during the Düzce earthquake was already seismically active after the Izmit earthquake.

Acknowledgements

We would like to thank two anonymous reviewers. Their constructive comments improved the manuscript. We thank Dino Bindi, Stefano Parolai for magnitude determination and Fatih Bulut for constructive discussions. Some figures were generated by the Generic Mapping Tools (GMT) code developed by Wessel and Smith (1991).

References

Aktar, M., Özalaybey, S., Ergin, M., Karabulut, H., Bouin, M. P., Tapirdamaz, C., Bicmen, F., Yörük, A., Bouchon, M., 2004. Spatial variation of aftershock activity across the rupture zone of the 17 August 1999 Izmit earthquake, Turkey, Tectonophysics, 391, 325-334.

Amitrano, D., 2003. Brittle-ductile transition and associated seismicity: Experimental and numerical studies and relationship with the b value, J. Geophys. Res., 108 (B1), 2044, doi:10. 1029/2001JB000680.

Barka, A., 1996. Slip distribution along the North Anatolian Fault associated with the large earthquakes of the period 1939 to 1967, Bull. Seism. Soc. Am., 86, 1238-1254.

Barka, A., Akyüz, H. S., Altunel, E., Sunal, G., Çakir, Z., Dikbas, A., Yerli, B., Armijo, R., Meyer, B., Chabalier, J. B. de, Rockwell, T., Dolan J. R., Hartleb, R., Dawson,

T., Christofferson, S., Tucker, A., Fumal, T., Langridge, R., Stenner, H., Lettis, W., Bachhuber, J. and Page, W., 2002. The Surface Rupture and Slip Distribution of the 17 August 1999 Izmit Earthquake (M 7.4, North Anatolian Fault, Bull. Seism. Soc. Am., 92(1), 43-60.

Baumbach, M. et al., 2003. Calibration of an Ml scale in the Northwestern Turkey from 1999 Izmit aftershocks, Bull. Seis. Soc. Am. 93(5), 2289-2295.

Bindi, D., Parolai, S., Görgün, E., Grosser, H., Milkereit, C., Bohnhoff, M. and Durukal, E., 2007. M_L Scale in Northwestern Turkey from 1999 Izmit Aftershocks: Updates, Bull. Seism. Soc. Am., 97, 331-338.

Bohnhoff M., Bulut, F., Görgün, E., Milkereit, C., Dresen, G., 2007. Seismotectonic setting at the North Anatolian Fault Zone after the 1999 Mw=7.4 Izmit earthquake based on high-resolution aftershock locations, Adv. Geosci., 14, 1-8, 2007.

Bouchon, M., Töksöz, M. N., Karabulut, H., Bouin, M. P., Dietrich, M., Aktar, M. & Edie M., 2002. Space and Time Evolution of Rupture and faulting during the 1999 Izmit (Turkey) Earthquake, Bull. Seism. Soc. Am., 92(1), 256-266.

Bulut, F., Bohnhoff, M., Aktar, M., Dresen, G., 2007. Characterization of aftershock-fault plane orientations of the 1999 Izmit (Turkey) earthquake using high-resolution aftershock locations, Geophys. Res. Lett., Vol. 34, L20306, doi: 10.1029/2007GL031154.

Bürgmann, R., Ergintav, S., Segall, P., Hearn, E.H., McClusky, S., Reilinger, R.E., Woith, H. and Zschau, J., 2002. Time-dependent Distributed Afterslip on deep below the Izmit Earthquake Rupture, Bull. Seism. Soc. Am., 92(1), 126-137.

Byerlee, J. D., 1970. Static and kinetic friction of granite under high stress. Int. J. Rock Mech. Min. Sci. 7 : 577-82.

Delouis, B., Giardini, C., Lundgren, P., and Salichon, J., 2002. Joint inversion of InSAR, GPS, Teleseismic and Strong-Motion Data for the Spatial and Temporal Distribution of Earthquake slip: Application to the 1999 Izmit Mainshock, Bull. Seism. Soc. Am., 92(1), 278-299.

Ishimoto, M., and Iida, K., 1939. Observations of earthquakes registered with the microseismograph constructed recently, Bull. Earthq. Res. Inst. 17, 443-478.

Gutenberg, R., and Richter, C. F., 1944. Frequency of earthquakes in California, Bull. Seism. Soc. Am., 34, 185-188.

Karabulut, H., Bouin, M. P., Bouchon, M., Dietrich, M., Cornou, C., Aktar, M., 2002. The seismicity in the Eastern Marmara Sea after the 17 August 1999 Izmit Earthquake. Bull. Seism. Soc. Am. 92: 387-393.

Lay, T., Kanamori, H., 1980. Earthquake doublets in the Solomon Islands. Phys.Earth Planet. Inter. 21:283-304.

Lay, T., Kanamori, H., 1981. An asperity model of great earthquake sequences. In Earthquake Prediction--An International Review, Maurice Ewing Ser., ed. D. W. Simpson, P. G. Richards, 4: 579-92. Washington DC : Am. Geophys. Union.

Lei, X., 2003. How do asperities fracture? An experimental study of unbroken asperities, Earth. and Plan. Scien. Lett., 213, 347-359.

McClusky, S., Balassanian, S., Barka, A., Demir, C., Ergintav, S., Georgiev, I., Gurkan, O., Hamburger, M., Hurst, K., Kahle, H., Kastens, K., Kekelidze, G., King, R., Kotzev, V., Lenk, O., Mahmoud, S., Mishin, A., Nadariya, M., Ouzounis, A., Paradissis, D., Peter, Y., Prilepin, M., Reilinger, R., Sanli, I., Seeger, H., Tealeb, A.,

Toksöz, M. N., and Veis, G., 2000. Global positioning system constraints on plate kinematics and dynamics in the eastern Mediterranean and Caucasus, J. Geophys. Res., 105, 5695-5719.

Milkereit, C., Zunbul, S., Karakisa, S., Iravul, Y., Zschau, J., Baumbach, M., Grosser, H., Gunther, E., Umutlu, N., Kuru, T., Erkul, E., Klinge, K., Ibs von Seht, M., Karaman, A., 2000. Preliminary aftershock analysis of M_w=7.4 Izmit and M_w=7.1 Düzce earthquake in Western Turkey. In: Barka, A., Ö. Kozaci, S. Akyüz (Editors): The 1999 Izmit and Düzce Earthquakes: preliminary results. ISBN: 975-561-182-7, pp. 179-187, Istanbul Technical University.

Mogi, K., 1962. Magnitude-frequency relation for elastic shocks accompanying fractures of various materials and some related problems in earthquakes, Bull. Earthquake Res. Inst., Univ. Tokyo, 40, 831-853.

Öncel, A.O. and Wyss, M., 2000. The major asperities of the 1999 M_w=7.4 Izmit earthquake defined by the microseismicity of the two decade before it, Geophys. J. Int., 143, 501-506.

Pucci, S., Palyvos, N., Zabci, C., Pantosti, D. and Barchi, M., 2006. Coseismic ruptures and tectonic landforms along the Düzce segment of the North Anatolian Fault Zone (Ms 7.1, November 1999), J. Geophys. Res., 111, B06312, doi:10.1029/2004JB003578.

Reilinger, R., Ergintav, S., Bürgmann, R., McClusky, S., Lenk, O., Barka, A., Gurkan, O., Hearn, L., Feigl, K. L., Cakmak, R., Aktug, B., Ozener, H., Töksoz, M. N., 2000. Coesmic and postseismic fault slip for the 17 August 1999, M=7.5, Izmit, Turkey earthquake, Science, 289, 1519-1524.

Reilinger, R. McClusky, S., Vernant, P., Lawrence, S., Ergintav, S., Cakmak, R., Ozener, H., Kadirov, F., Guliev, I., Stepanyan, R., Nadariya, M., Hahubia, G., Mahmoud, S., Sakr, K., ArRajehi, A., Paradissis, D., Al-Aydrus, A., Prilepin, M., Guseva, T., Evren, E., Dmitrotsa, A., Filikov, S. V., Gomez, F., Al-Ghazzi, R., Karam, G., 2006. GPS constraints on continental deformation in the Africa-Arabia-Eurasia continental collision zone and implications for the dynamics of plate interactions, J. Geophys. Res., 111, B05411, doi:10.1029/2005JB004051.

Schorlemmer, D., Neri, G., Wiemer, S. and Mostaccio A., 2003. Stability and significance tests for b-value anomalies: Example from the Tyrrhenian Sea, Geophys. Res. Lett., 30(16), 1835, doi:10.1029/2003GL017335.

Schorlemmer, D., Wiemer, S., Wyss, M., 2004. Earthquake statistics at Parkfield: 1. Stationary of *b* values, J. Geophys. Res., 109, B12307, doi:10.1029/2004JB003234.

Schorlemmer, D. and Wiemer, S., 2005. Microseismicity data forecast rupture area, Nature, 434, 1086.

Schorlemmer, D., S. Wiemer, and M. Wyss, 2005. Variations in earthquake-size distribution across different stress regimes, Nature, 437, 539-542, doi: 10.1038/nature04094.

Scholz, C. H., 1968. The frequency-magnitude relation of microfracturing in rock and its relation to earthquakes, Bull. Seismol. Soc. Am., 58, 399-415.

Scholz, C. H., Engelder, J. T., 1976. The role of asperity indentation and ploughing in rock friction-1. Asperity creep and stick-slip. Int. J. Rock. Mech. Min. Sci. Geomech.13:149-54 (Abstr.).

Sobiesiak, M., Meyer, U., Schmidt, S., Götze, H.-J., and Krawczyk, C. M., 2007. Asperity generating upper crustal sources revealed by *b* value and isostatic residual anomaly grids in the area of Antofagasta, Chile, J. Geophys. Res., 112, B12308, doi:10.1029/2006JB004796.

Şaroğlu, F., Ö. Emre, and I. Kuşcu, Active Fault Map of Turkey, General Directorate of Mineral Research and Exploration (MTA), Eskisehir Yolu, 06520, Ankara, Turkey, 1992.

Steacy, S. J. and McCloskey, J., 1998. What controls an earthquake's size? Results from a heterogeneous cellular automaton, Geophys. J. Int., 133**,** f11–f14.

Tibi, R., Bock, G., Xia, Y., Baumbach, M., Grosser, H., Milkereit, C., Karakisa, S., Zunbul, S., Kind, R., Zschau, J., 2001. Rupture processes of the 1999 August 17 Izmit and November 12 Düzce (Turkey) earthquakes, Geophys. J. Int., 144, F1-F7.

Utkucu, M., Nalbant, S. S., McCloskey, J., Steacy, S. and Alptekin, Ö., 2003. Slip distribution and stress changes associated with the 1999 November 12, Düzce earthquake (M_w = 7.1), Geophys. J. Int., 153, 229-241.

Utsu, T., 1961. A Statistical study on the occurrence of aftershocks, Geophys. Mag., Tokyo, 30, 521-603, Japan.

Utsu, T., 1966. A Statistical Significance Test of the Difference in b Value Between Two Earthquake Groups, J. Phys. Earth 14, 37–40.

Utsu, T., 1999. Representation and analysis of the earthquake size distribution: a historical review and some new approaches, Pageoph 155, 509–535.

Wessel, P., Smith, W.H.F., 1991. Free software helps map and display data. EOS, Trans., Am. Geophys. Union 72, 445–446.

Westerhaus, M., Wyss, M., Yilmaz, R. and Zschau, J., 2002. Correlating variations of b values and crustal deformations during the 1990s may have pinpointed the rupture initiation of the Mw=7.4 Izmit earthquake of 1999 August 17, Geophys. J. Int., 148, 139-152.

Wiemer, S. and Wyss, M., 1997. Mapping the frequency-magnitude distribution in asperities: An improved technique to calculate recurrence times?, J. Geophys. Res., 102, 15115-15128.

Wiemer, S., and Katsumata, K., 1999. Spatial variability of seismicity parameters in aftershock zones, J. Geophys. Res., 104, 13135-13151.

Wiemer, S., 2001. A software package to analyze seismicity: ZMAP, Seis. Res. Lett., 72(2), 374-383.

Wiemer, S., and Wyss M., 2002. Mapping spatial variability of the frequency-magnitude distribution of earthquakes, Adv. Geophys., 45, 259– 302.

Woessner, J. and Wiemer, S., 2005. Assessing the quality of earthquake catalogues: Estimating the magnitude of completeness and its uncertainty, Bull. Seismol. Soc. Am., 95, 684-698.

Wright, T., Fielding, E. and Parsons, B., 2001. Triggered slip: observations of the 17 August 1999 Izmit (Turkey) earthquake using radar interferometry, Geophys. Res. Lett., 28, 1079-1082.

Wyss, M., Sammis, C. G., Nadeau, R. M., and Wiemer, S., 2004. Fractal dimension and b-value on creeping and locked patches of the San Andreas Fault near Parkfield, California, Bull. Seismol. Soc. Am., 94, 410.

Zang, A., Wagner, F. C., Stanchits, S., Dresen, G., Andresen, R. and Haidekker, M., 1998. Source analysis of acoustic emissions in Aue granite cores under symmetric compressive loads, Geophys. J. Int., 135, 1113-1130.

Figure Captions

Figure 1: a) Topographic map of the North Anatolian Fault Zone (NAFZ) region (Şaroğlu et al., 1992). Black arrows indicate the GPS-derived surface displacement rate (McClusky et al., 2000; Reilinger et al., 2006). b) Izmit-Düzce segment of the NAFZ. Red lines indicate the Izmit 1999 surface rupture as mapped by Barka et al. (2002) and blue line indicates the Düzce 1999 surface rupture trace as mapped by Pucci et al. (2006). Hypocenters of the 1999 Izmit (blue) and Düzce (red) earthquakes are indicated by stars. Maximum surface displacement observed (5.2 m) is located in the Sapanca - Akyazi segment. In the Izmit-Sapanca Lake segment, the maximum surface displacement observed is 3.5 m and in the Karadere segment 1.5 m.

Figure 2: Colored circles represent Izmit aftershock epicenters along the rupture of the mainshock as recorded by the seismic network (yellow triangles = SABONET stations). Event magnitudes are shown by different sized and colored circles. For reference, the Izmit $M_w = 7.4$ and the Düzce $M_w = 7.2$ strike-slip focal mechanisms are plotted (Tibi et. al, 2001). In (b) the depth section of aftershock hypocenters is plotted.

Figure 3: Black line indicates time variation of the M_c threshold estimated for the catalog. Dashed lines represent standard deviation of M_c.

Figure 4: a) Surface map view of standard deviations in *b*-values for the catalog using bootstrap approach. b) Map view of *b*-values for SC and KDC. Black crosses represent

Izmit aftershocks. c) Frequency-magnitude distributions for the marked regions in frame (b).

Figure 5: a) Cross-section of standard deviations in *b*-values for the catalog using bootstrap approach. b) *b*-value cross-section of the SC and KDC. Hypocenters are marked with black crosses. c) Last 25 days postseismic slip rate derived from GPS by Bürgmann et al. (2002).

Figure 6: *b*-value as a function of depth for (a) SC and (b) KDC. The *b*-values are calculated using 50 events in the vertically sliding windows. Squares mark the center of the window, vertical lines show the window size and horizontal lines show the standard deviation of *b*-value.

Figure 7: Topographic map view of Izmit aftershocks (black circles) at Karadere-Düzce region. Red star indicates the Düzce hypocenter (November 12, 1999). Red line represents the Karadere fault which was ruptured during Izmit coseismic period (Barka et al., 2002). Blue dashed line indicates the Düzce surface rupture according to Pucci et al (2006).

Figure 8: From *b*-value analysis in Figure 4 we find three asperity regions (Asperity 1, Asperity 2 and Asperity 3). The red line indicates the surface rupture of the August 17, 1999 Izmit earthquake (Barka et al., 2002). The blue line is the surface rupture of the November 12, 1999 Düzce earthquake (Pucci et al., 2006).

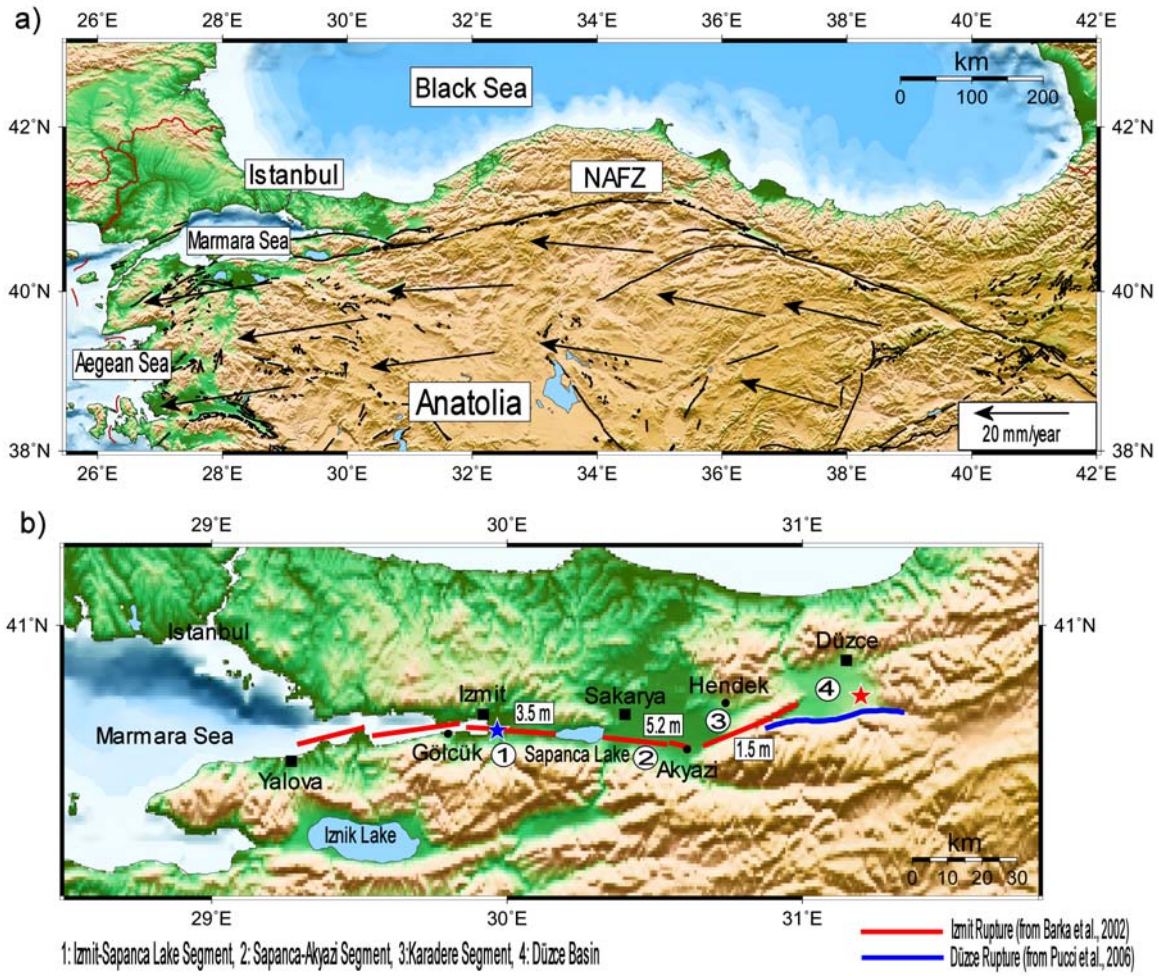
a)
26°E
28°E
30°E
32°E
34°E
36°E
38°E
40°E
42°E
42°N
40°N
38°N
Black Sea
km
0
100
200
Istanbul
NAFZ
Marmara Sea
Aegean Sea
Anatolia
20 mm/year
b)
29°E
30°E
31°E
41°N
Istanbul
Düzce
Izmit
Sakarya
Hendek
3.5 m
5.2 m
1.5 m
Marmara Sea
Gölcük
Sapanca Lake
Akyazi
Yalova
Iznik Lake
km
0
10
20
30
1: Izmit-Sapanca Lake Segment, 2: Sapanca-Akyazi Segment, 3:Karadere Segment, 4: Düzce Basin
Izmit Rupture (from Barka et al., 2002)
Düzce Rupture (from Pucci et al., 2006)

Figure 1

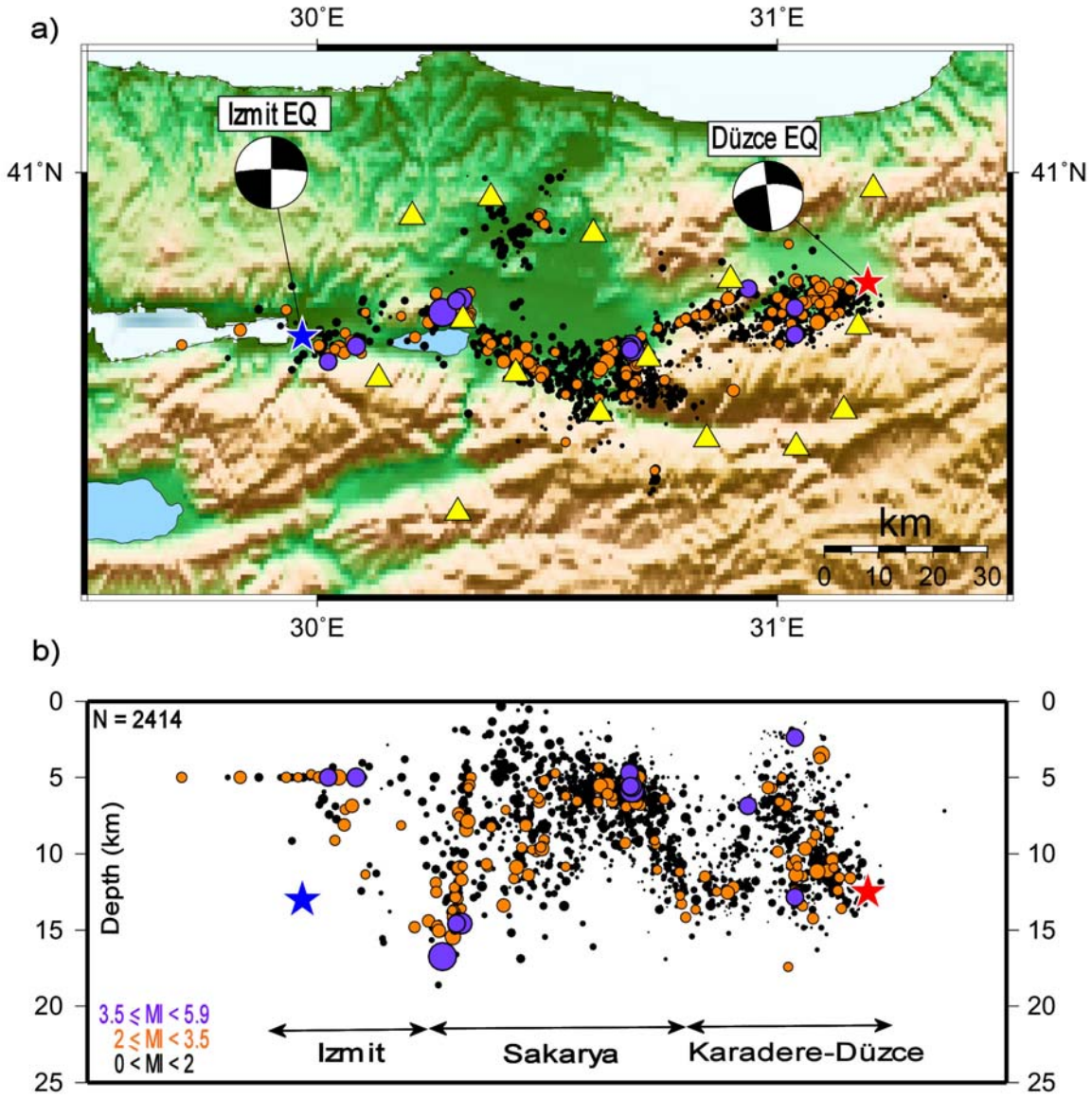
a)
30°E
31°E
41°N
İzmit EQ
Düzce EQ
km
0 10 20 30
b)
N = 2414
Depth (km)
3.5 ≤ Ml < 5.9
2 ≤ Ml < 3.5
0 < Ml < 2
İzmit
Sakarya
Karadere-Düzce

Figure 2

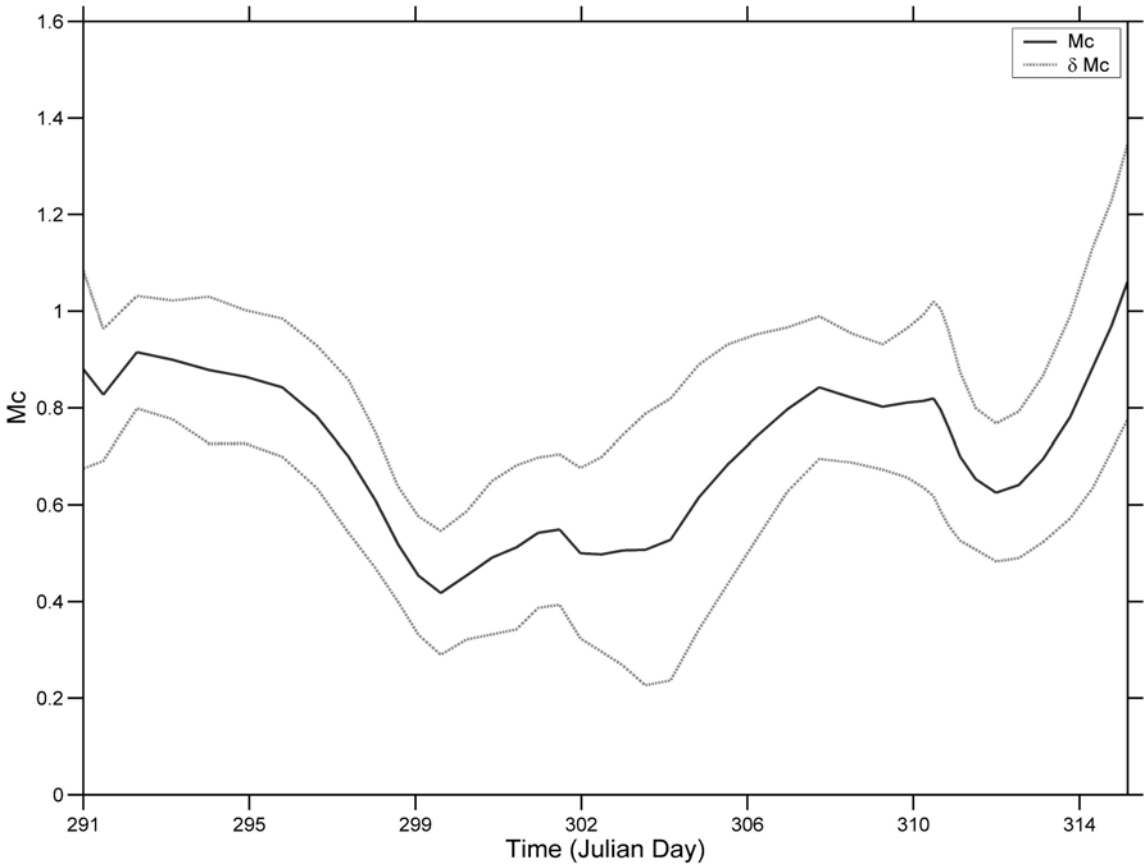
Mc
δ Mc
1.6
1.4
1.2
1
0.8
0.6
0.4
0.2
0
Mc
291
295
299
302
306
310
314
Time (Julian Day)

Figure 3

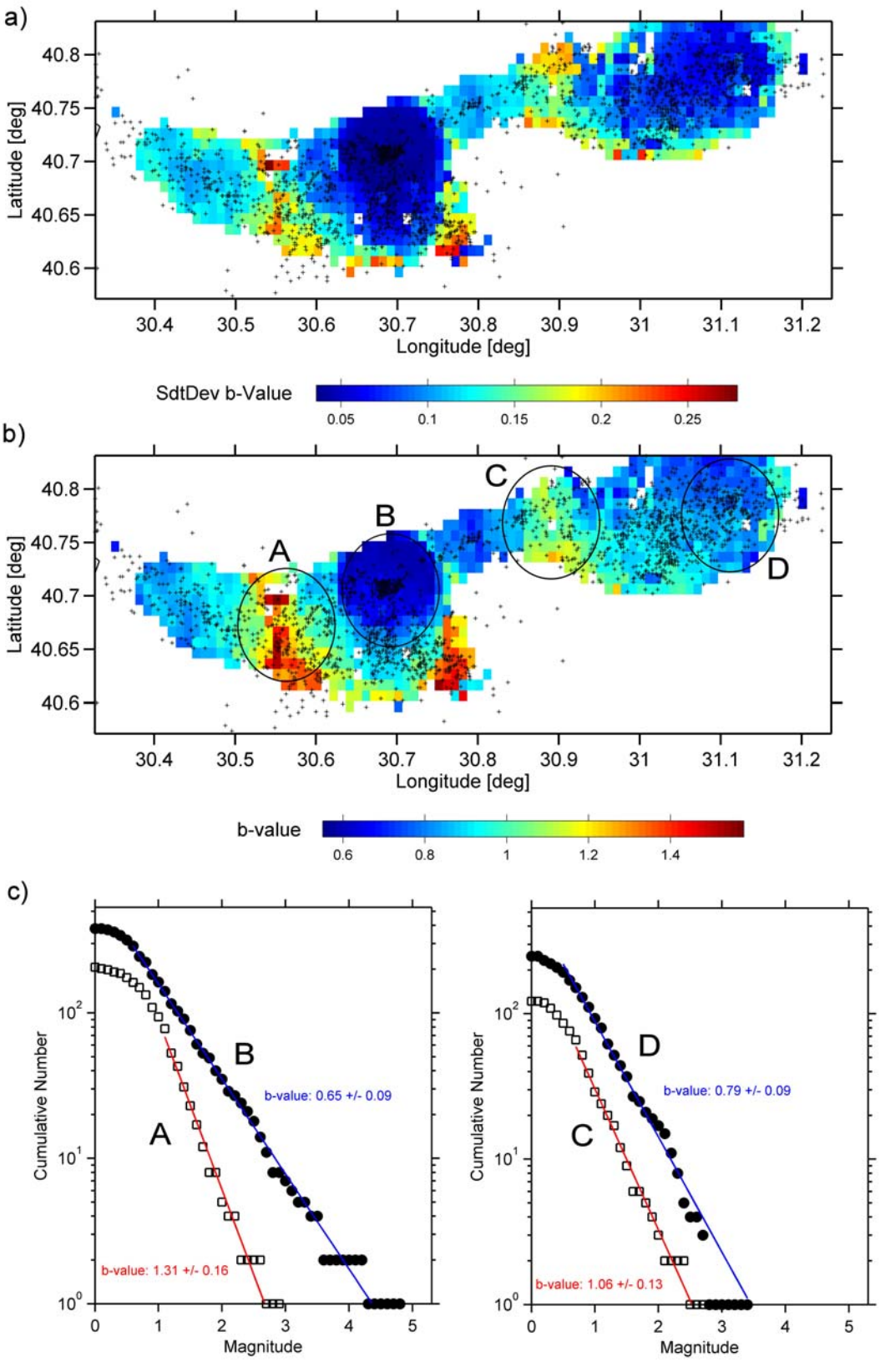
a)
Latitude [deg]
40.8
40.75
40.7
40.65
40.6
30.4
30.5
30.6
30.7
30.8
30.9
31
31.1
31.2
Longitude [deg]
SdtDev b-Value
0.05
0.1
0.15
0.2
0.25
b)
A
B
C
D
b-value
0.6
0.8
1
1.2
1.4
c)
Cumulative Number
Magnitude
b-value: 0.65 +/- 0.09
b-value: 1.31 +/- 0.16
b-value: 0.79 +/- 0.09
b-value: 1.06 +/- 0.13

Figure 4

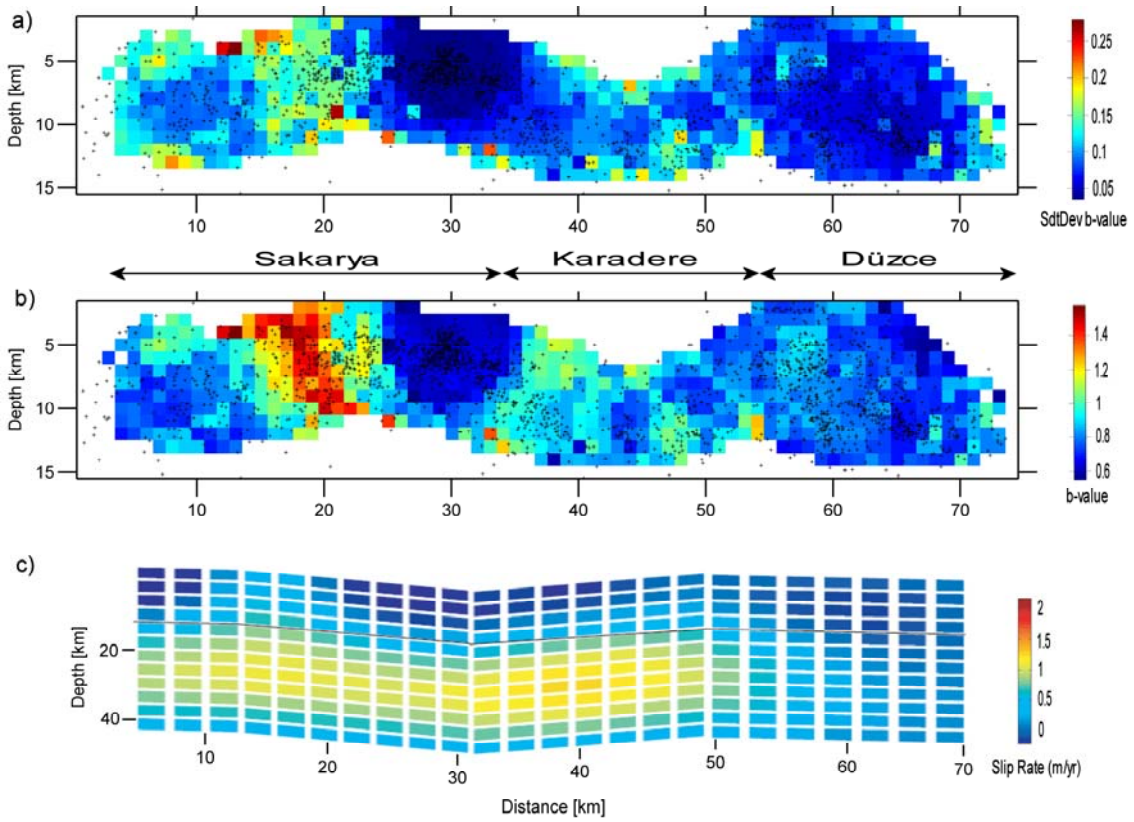
a)
Depth [km]
5
10
15
10
20
30
40
50
60
70
0.25
0.2
0.15
0.1
0.05
SdtDev b-value
Sakarya
Karadere
Düzce
b)
Depth [km]
5
10
15
10
20
30
40
50
60
70
1.4
1.2
1
0.8
0.6
b-value
c)
Depth [km]
20
40
10
20
30
40
50
60
70
2
1.5
1
0.5
0
Slip Rate (m/yr)
Distance [km]

Figure 5

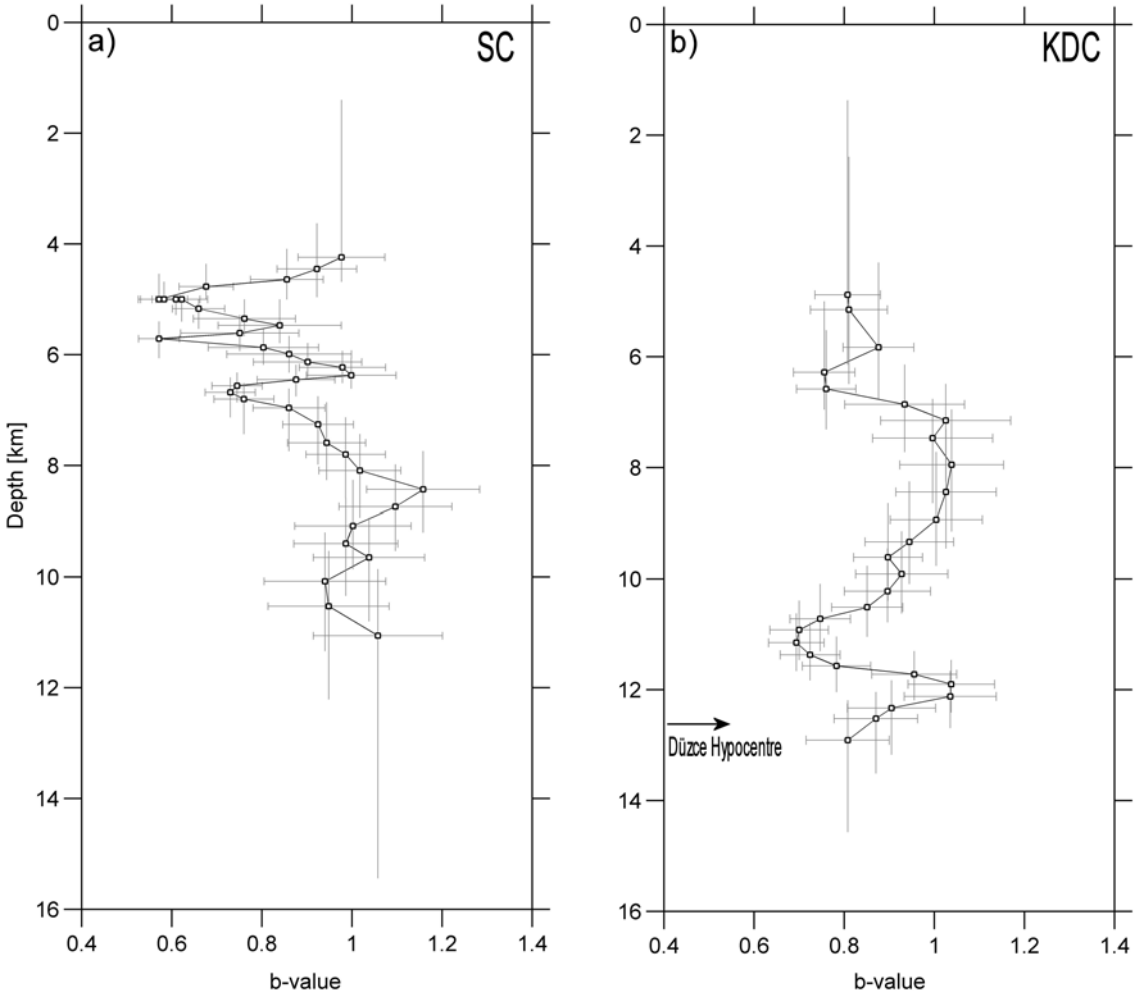
a)
SC
b)
KDC
Depth [km]
b-value
b-value
Düzce Hypocentre
0
2
4
6
8
10
12
14
16
0.4
0.6
0.8
1
1.2
1.4

Figure 6

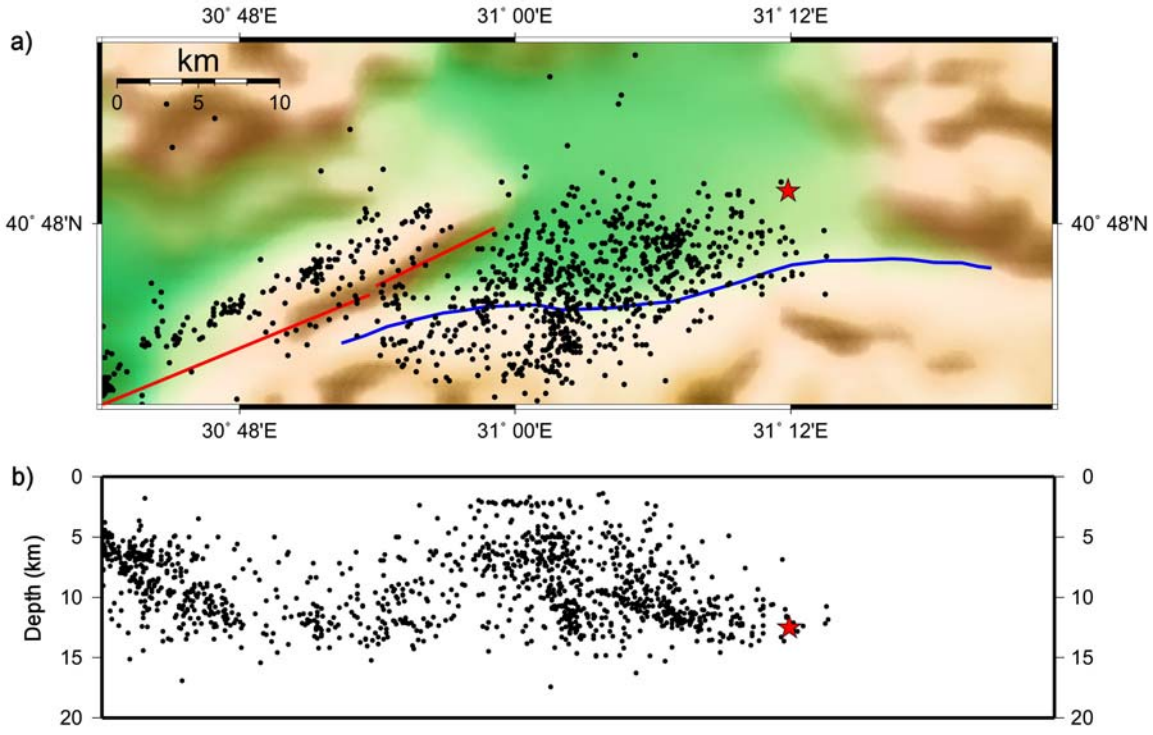

Figure 7

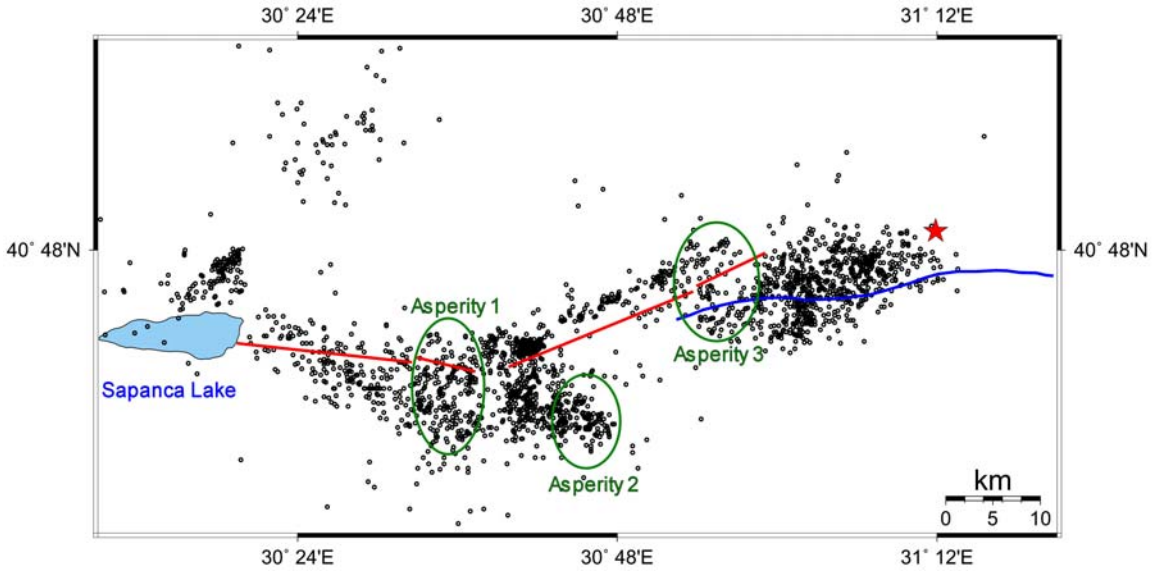
30° 24'E
30° 48'E
31° 12'E
40° 48'N
40° 48'N
Asperity 1
Asperity 3
Sapanca Lake
Asperity 2
km
0 5 10
30° 24'E
30° 48'E
31° 12'E

Figure 8